

## Structural controls on rare-metal mineralization: Depth-specific mapping of economic deposits in Nigeria Basement Complex

E. Abraham<sup>1\*</sup>, M. Abdulfarraj<sup>2</sup>, M. Emetere<sup>3</sup>, A. Usman<sup>1</sup>, I. Ikeazota<sup>1</sup>

<sup>1</sup>Alex Ekwueme Federal University, Ikwo, Nigeria

<sup>2</sup>Abdulaziz University, Jeddah, Saudi Arabia

<sup>3</sup>Bowen University, Iwo, Nigeria

\*Corresponding author: [ema.abraham@funai.edu.ng](mailto:ema.abraham@funai.edu.ng)

**Abstract.** This study aims to identify prospective zones for mineral exploration and enhance understanding of mineralization processes within Precambrian terrains. High-resolution aeromagnetic data were analyzed using integrated geophysical techniques such as Analytic Signal, Tilt Derivative, Phase Symmetry, Source Parameter Imaging, Butterworth bandpass filtering, 3D magnetic anomaly inversion, and Euler Deconvolution to delineate subsurface structures and determine their spatial distribution, depths, and relationships to mineral occurrences. The results revealed NE-SW and NW-SE trending lineaments corresponding to major shear zones and fault systems that govern mineral emplacement. Shallow sources (250-500 m) are associated with industrial minerals such as clay, intermediate depths (500-720 m) relate to rare-metal pegmatites hosting columbite-tantalite and wolframite, while deep-seated structures (>1200 m) indicate potential source regions for mineralizing fluids. High-amplitude analytic signal anomalies (0.04-0.05 nT/m) coincide with geological contacts and structural boundaries marking zones of potential mineralization. This represents the first comprehensive investigation of subsurface mineralized structures in the region, and by applying multiple geophysical processing techniques, previously unmapped structural features were exposed and the vertical continuity of mineralized zones confirmed. The findings provide depth-specific mapping of economic mineral deposits, offering valuable insights for targeted exploration efforts and enabling more precise, cost-effective strategies for locating columbite-tantalite, wolframite, kaolin, and other economically significant minerals in the Basement Complex.

**Keywords:** magnetic data, minerals exploration, depths, structural controls, mining, basement complex.

Received: 20 March 2025

Accepted: 7 November 2025

Available online: 30 December 2025

### 1. Introduction

Variations in magnetic field of the earth at some regions can indicate the presence of certain mineral deposits or geological structures. Exploration and discovery of mineral resources play a crucial role in the economic development of nations [1], particularly in regions with untapped geological potential. In recent years, advanced geophysical techniques have revolutionized the field of mineral exploration, offering more precise and cost-effective methods for identifying promising deposits [2-7]. Among these techniques, the analysis of magnetic anomaly signatures has emerged as a powerful tool for unraveling the hidden subsurface mineralized structures of economic value [5].

Nigeria, with its diverse geological landscape, is recognized for its mineral resource potential [7]. However, large areas of the country, particularly within the Precambrian Shield regions, remain underexplored. The Kaduna-Nasarawa region, situated within the Nigerian Precambrian Basement Complex, represents one such promising yet understudied region [7]. This area, characterized by its ancient rock formations and complex tectonic history is itself a segment of the

West African Craton and holds significant potential for various mineral deposits, including clay, columbite, garnet kaolin/kaolinitic clay, mica, talc, tantalite, tourmaline, wolframite, iron ore, gold, and rare earth elements [8, 9]. Recent advancements in magnetic survey technologies and data interpretation methods have opened new avenues for understanding the subsurface geology of such complex terrains [2-4]. By detecting subtle variations in the magnetic field anomalies caused by differences in rock magnetization, these techniques have revealed valuable information about underlying geological structures and potential mineralization zones [5].

Over the past few decades, several studies [10, 11] have been conducted to explore the mineral potentials and geological characteristics of this region. These studies have utilized various geological and geophysical techniques to understand the structural framework and mineralization processes within the basement complex. The ability to detect magnetic field variations in the Earth, caused by subsurface magnetic minerals such as magnetite and ilmenite presents magnetic surveys as essential tools for exploring basement complex terrains [12]. These variations of magnetic anomalies, are key

indicators of geological structures, such as faults, fractures, intrusions and shear zones, which often serve as conduits for mineralizing fluids. In the Kaduna-Nasarawa Precambrian Shield (KNPS), interpreting these magnetic anomalies can reveal hidden mineral deposits and provide insights into the structural controls governing mineralization. However, despite the recognized mineral potential of this region, detailed geophysical studies to delineate these subsurface structures, depth extents and trends are relatively limited, necessitating the need for this study. This study will shed light on the enclosed geological features of the Kaduna-Nasarawa region, paving the way for a more targeted and efficient mineral exploration efforts in the region. The area under investigation is basically parts of four states, Kaduna, Nasarawa, Plateau and Bauchi States of northern Nigeria and covers an area of 18150 km<sup>2</sup>. It is bounded by Longitudes 8°00'-9°30' E and Latitudes 9°00'-10°00' N (Figure 1).

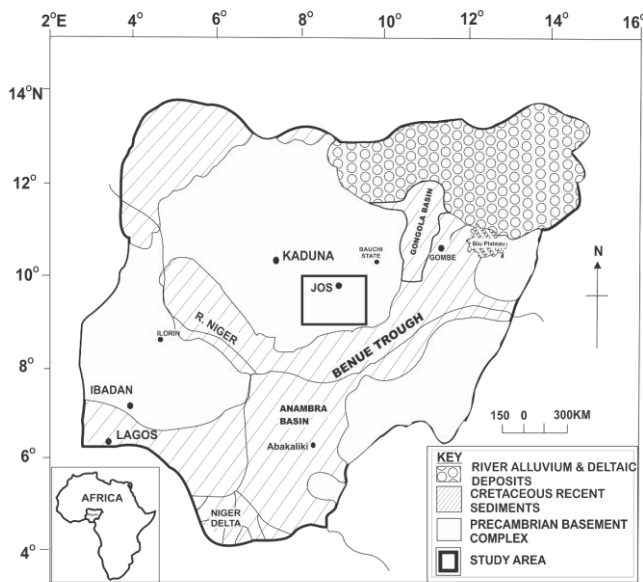


**Figure 1. Map of Nigeria. The map also displays an overview geological setup within the region (modified from [2])**

Early geological mapping efforts, such as those by McCurry [11] and Rahaman [10], provided a foundational understanding of the lithological composition and structural features of the region. These studies highlighted the presence of various rock types, including syenite, quartz, gabbro, migmatites, gneisses, schists, and granitoids, and emphasized the importance of fault systems in controlling mineralization. Subsequent geochemical surveys, conducted by Ogezi [9] and other researchers, identified significant concentrations of tin, columbite, gold, and other minerals, particularly in association with the Younger Granites of the Jos Plateau and quartz veins within the schist belts. Woakes et al. [13] demonstrated the utility of aeromagnetic data in revealing the structural framework of the Crystalline Basement Complex of Nigeria and its influence on mineralization. These studies showed that major fault systems, trending NE-SW, NW-SE, and E-W, are key structural features that control the emplacement of mineral-rich fluids, thereby influencing the distribution of mineral deposits [7]. Although these studies have provided insights into the region's geology, they have often been limited by reach and resolution of the data leaving significant gaps in the understanding of the subsurface geology and mineralization processes of the basement complex.

Other previous investigations relied on surface mapping, which may not fully capture the complexity of the subsurface structures and their role in mineralization. Moreover, the region's challenging terrain and dense vegetation often make traditional geological mapping difficult, further complicating efforts to accurately delineate mineral deposits. There is a pressing need for a more comprehensive geophysical approach that can provide higher resolution data and better constrain the subsurface structures and mineralization zones [2, 4, 5, 12].

Despite the mineral potential of the study area, comprehensive geophysical exploration remains limited. However, some insights have been provided by Ugwu et al. [14], who analyzed aeromagnetic data in the Jos Plateau region, which encompasses a smaller part of our study area. Their analysis revealed distinct structural lineaments oriented in multiple directions: northeast-southwest (NE-SW), northwest-southeast (NW-SE), east-west (E-W), and north-south (N-S). These structural trends were interpreted as potential fault and fracture systems, suggesting a complex tectonic history that may have influenced mineralization patterns in the region. The correlation between these structural trends and mineral occurrences, warrants further investigation through integrated geophysical approaches. Our study aims to investigate the magnetic anomaly signatures within the KNPS and their implications for mineral exploration. We seek to identify and characterize promising areas for further exploration efforts through the integration of high-resolution aeromagnetic data with geological information. The increasing demand for sustainable mining practices and the need to optimize exploration strategies to minimize environmental impact and maximize economic benefits in the mining and exploration industry makes this study very timely.

### 1.1. Geological setting

The Kaduna-Nasarawa region is situated within the Nigerian Precambrian Basement Complex, a crucial component of the Trans-Saharan Belt (TSB) of West Africa [15]. This belt, extending from Algeria through Niger and Nigeria to Benin, represents a major Pan-African orogeny that occurred during the late Neoproterozoic to early Cambrian period (ca. 600-540 Ma) [16]. The Nigerian Basement Complex, covering approximately half of Nigeria's landmass, plays a pivotal role in understanding the region's tectonic evolution and mineralization potential [7]. This complex is characterized by a diverse assemblage of metamorphic and igneous rocks, primarily of Precambrian age and is broadly divided into three major lithological units (Figure 2):

1. **Migmatite-Gneiss Complex**; which forms the basement sensu stricto and is considered to be Archean to Early Proterozoic in age (>2000 Ma). It also consists of high-grade gneisses, migmatites, and local occurrences of meta-supracrustal rocks [17].

2. **Schist Belts**; which are predominantly metasedimentary and metavolcanic rocks of Late Proterozoic age (900-600 Ma). They occur as N-S trending belts within the Migmatite-Gneiss Complex and are interpreted as ancient sedimentary basins that were deformed and metamorphosed during the Pan-African orogeny [18].

3. **Older Granites**; which are Pan-African intrusive suites emplaced during the late Neoproterozoic to early Cambrian (750-450 Ma). They range in composition from tonalite to granite and are typically unfoliated to weakly foliated [19].

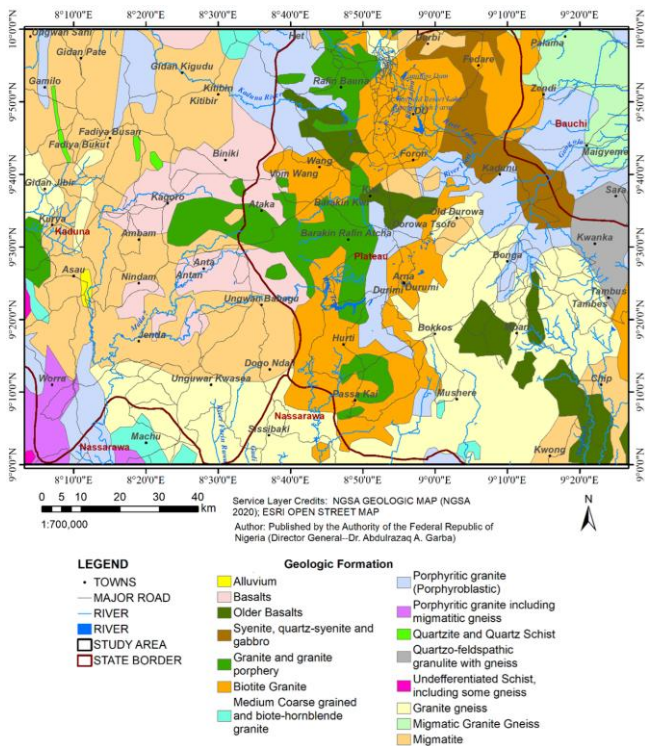


*Figure 2. Geologic map of the study area (Map was extracted from the Nigerian Geological Survey Agency [8])*

The Kaduna-Nasarawa area specifically straddles the boundary between the Migmatite-Gneiss Complex and the Schist Belts, providing a unique geological setting with potential for various mineralization styles. The dominant lithologies in the Kaduna-Nasarawa region are the Migmatitic gneisses that forms the basement rocks and are composed of quartzo-feldspathic minerals with variable amounts of biotite and hornblende (Figure 2). Complex folding and banding patterns, with leucosomes of granitic composition and melanosomes rich in mafic minerals are noticeable [10]. Predominant quartz-mica schists, with occasional occurrences of graphitic and calc-silicate schists has also been recorded and they typically contain quartz, muscovite, and biotite as major minerals, with garnet, staurolite, and kyanite as common metamorphic index minerals indicating amphibolite facies metamorphism [20]. Amphibolites occur as concordant bands within the gneisses and schists, and often associated with meta-ultramafic bodies. They are composed mainly of hornblende and plagioclase, with minor amounts of quartz, biotite, and epidote. Some amphibolites may represent metamorphosed mafic volcanic rocks or intrusions [21]. Occurring as resistant ridges, are quartzites which are often ferruginous and may host significant iron mineralization. They are composed predominantly of quartz with minor amounts of muscovite, biotite, and magnetite. The ferruginous quartzites, also known as banded iron formations (BIFs), consist of alternating bands of iron-rich (mainly hematite and magnetite) and silica-rich layers [22]. The granitoids include both the Older Granites (Pan-African) and younger intrusive bodies and they range in composition from granodiorite to syenite. The Older Granites are typically porphyritic, with large K-feldspar phenocrysts in a matrix of quartz, plagioclase, biotite, and hornblende. Younger intrusions include pegmatites, which are often associated with rare metal mineralization [23]. Meta-ultramafic rocks (although less common),

occur as small bodies within the schist belts and are composed mainly of serpentinized peridotites and pyroxenites. They may represent remnants of oceanic crust and could be associated with nickel and chromium mineralization [24].

The KNPS region has undergone multiple phases of deformation, resulting in a complex structural framework. Some of the key structural features are the NNE-SSW trending foliation, which is the dominant structural grain in the area. This foliation is associated with the main phase of the Pan-African orogeny and is particularly well-developed in the schists and gneisses [25]. The tight to isoclinal folds, often with axial planar cleavage and typically associated with the deformation phase having axes that plunge gently to moderately towards the NNE or SSW [26]. The shear zones and faults, some of which may control mineralization. Major shear zones in the region trend NE-SW and NW-SE, and often show evidence of multiple reactivation events. These structures have been noted to host significant gold mineralization, particularly where they intersect favorable lithologies [27]. Late-stage brittle fractures and joints, which often trend E-W and may be related to Mesozoic rifting events associated with the break-up of Gondwana [28]. Mylonitic zones, particularly along the margins of granitic intrusions, indicating high-strain deformation during the emplacement of the Older Granites [23]. Okonkwo and Folorunso [30] showed that the Migmatite-Gneiss Complex typically shows evidence of high-grade metamorphism, reaching upper amphibolite to granulite facies conditions ( $T = 650\text{--}800^\circ\text{C}$ ;  $P = 6\text{--}10\text{ kbar}$ ) and the Schist Belts generally exhibit lower to middle amphibolite facies metamorphism ( $T = 500\text{--}650^\circ\text{C}$ ;  $P = 4\text{--}7\text{ kbar}$ ), with local variations depending on proximity to intrusive bodies.

Therefore, the geological setting of the KNPS region provides favorable conditions for various types of mineralization (Figure 3) to include: Gold, which usually associated with quartz veins in shear zones within the schist belts and may be related to hydrothermal activity during the late stages of the Pan-African orogeny [18].

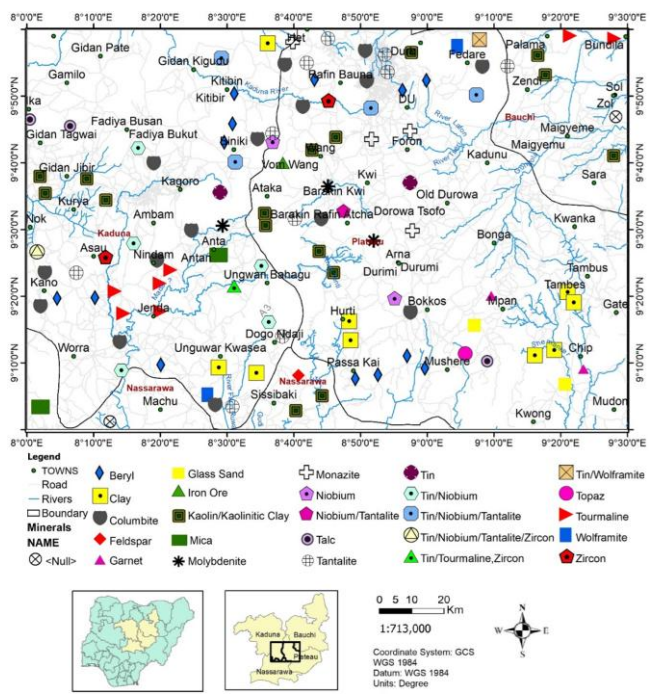


*Figure 3. Mineral resources map of the study area (extracted from Mineral map of Nigerian Geological Survey Agency [8])*

Iron ore hosted in banded iron formations and ferruginous quartzites known to contain significant reserves of hematite and magnetite [22]. Rare Earth Elements (REE) which are potentially concentrated in pegmatites and alkaline granites. The pegmatites also host significant tantalum and niobium mineralization (Figure 3) [29]. Gemstones including beryl (aquamarine, emerald) and tourmaline in pegmatitic bodies, particularly those associated with the younger granitic intrusions. Nickel and Chromium, potentially associated with the meta-ultramafic bodies. Although economic deposits of nickel and chromium have not yet been ascertained in the region, we believe this study would provide ample information of the structures within the suspected regions for further assessments and action.

Other mineral occurrences have been documented in the region. Some of them includes Clay and Kaolinitic Clay (Figure 3), which are widely distributed throughout the region, and are primarily derived from the weathering of feldspar-rich rocks such as granites and gneisses. The quality and quantity of these clay deposits make them potential resources for the ceramics and paper industries. Columbite and Tantalite also recorded in the N, NW and southern regions are often referred to collectively as coltan and are found in the pegmatites associated with the Older Granite suite. They typically occur as accessory minerals in pegmatites, often in association with cassiterite (tin ore).

## 1.2. Mineral setting

The Nasarawa area, in particular, has been noted for its columbite-tantalite mineralization, which is part of the larger Jos Plateau tin field (Figure 3). Garnets are common in the metamorphic rocks of the region (Kwi location), particularly in the higher-grade gneisses and schists. Almandine garnet is the most common variety, often found in garnet-mica schists and as porphyroblasts in gneisses [21]. While most occurrences are of mineralogical interest, some deposits may be of gem quality. Various types of mica, including muscovite and biotite, are abundant in the region's Older Granitoid rocks (SE region). Large mica books, of potential economic interest, are primarily associated with pegmatites [18]. The Older Granite pegmatites in particular have been known to host significant mica deposits. Talc deposits in the region are typically associated with ultramafic bodies that have undergone hydrothermal alteration. These deposits often occur as talc-schists or steatite bodies within the metavolcanic sequences of the schist belts [20]. The quality and extent of these deposits vary, with some potentially suitable for industrial applications. Tourmaline mineral is commonly found in the pegmatites of the region, often in association with other rare-metal mineralization. Tourmaline in the Kaduna-Nasarawa area ranges from common schorl to gem-quality elbaite varieties [30].

Some pegmatites in the region have yielded gem-quality tourmalines of various colors. While Wolframite is less common than some of the other minerals documented in the region, it has been reported at the NE region of the study area (Palama location) (Figure 3) and typically associated with quartz veins in granitic and metamorphic terrains [18]. We believe the distribution of these minerals is closely tied to the regional geology as the pegmatites, particularly those associated with the Older Granites, are the primary hosts for columbite, tantalite, beryl, tourmaline, and some high-quality mica deposits. The metamorphic rocks, especially the schists

and gneisses, host the garnet and some of the mica occurrences (Figure 3). Clay and kaolinitic clay deposits are found in the weathered profiles developed over feldspar-rich basement rocks in the Central region of the study area. Talc deposits are associated with ultramafic bodies within the schist belts found in the NW and SE regions.

## 2. Methods

For this investigation, we analyzed magnetic field data collected during an extensive aerial survey of Nigeria. Fugro Airborne Surveys conducted the fieldwork from 2005-2009 under the direction of the Nigerian Geological Survey Agency (NGSA). The aircraft maintained 500 m spacing between flight lines while traveling northwest to southeast at 80 meters above ground level. After collection, the data was organized into gridded maps, with each grid covering a half-degree square area.

To ensure high data quality, the team accounted for both regional magnetic field variations and daily fluctuations. The magnetic measurements underwent Reduction to Equator (RTE) processing following established methodologies [2], [31]-[36]. This mathematical transformation, performed using fast Fourier transform algorithms, incorporated the local magnetic parameters:  $-2.15^\circ$  declination and  $-13.91^\circ$  inclination. The final processed aeromagnetic data appears in Figure 4.

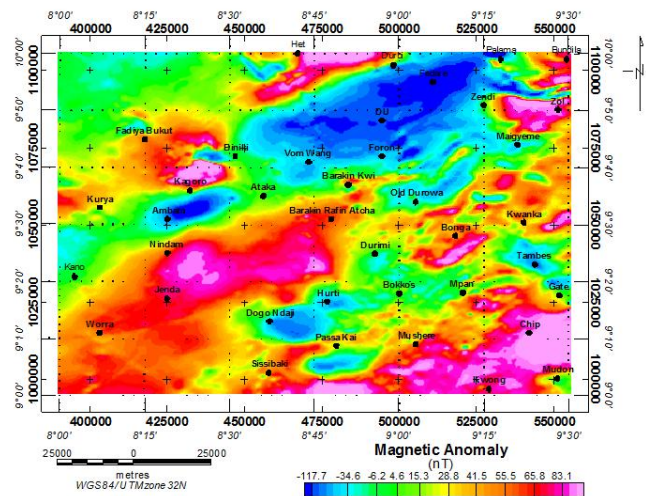


*Figure 4. Residual aeromagnetic anomaly map*

The map displayed notable variations in magnetic intensity, reflecting a range of distinct magnetic properties. High positive magnetic anomalies ( $>84.1$  nT) are spotted around Chip, Zol, Het and Jenda locations. These regions are traced to the granites and older basalts of the Precambrian basement complex and indicates the presence of high magnetic mineral at these locations. Significant lower magnetic anomalies ( $<-115$  nT) are noticeable in the northern and NE regions of the study area and is traced to the highly fractured and porphyritic granite formation in the locations.

## 2.1. Source parameter imaging (SPI)

Magnetic source depth estimation has been enhanced by the SPI method, which automatically analyzes gridded magnetic data. Unlike traditional approaches, SPI functions effectively regardless of magnetic inclination and declination values, making pole reduction unnecessary during analysis [2]. Recent field testing with drill-confirmed data sources

shows that SPI consistently achieves depth predictions within  $\pm 20\%$  accuracy, matching the precision of established methods like Euler deconvolution. Nevertheless, SPI surpasses Euler deconvolution by producing more extensive and internally consistent solution sets, enabling a better visualization of underground formations.

The theoretical foundation of SPI rests on a step-source model [37]. This model is governed by the following mathematical relationship:

$$Depth = 1 / K_{\max} , \quad (1)$$

where:  $K_{\max}$  is the peak value of the local wavenumber  $K$  over the step source.

$$K = \sqrt{\left(\frac{dA}{dx}\right)^2 + \left(\frac{dA}{dy}\right)^2}, \quad (2)$$

where:

$$Title\ derivative\ A = \tan^{-1} \left\{ \frac{\left[ \frac{dM}{dz} \right]}{\left( \frac{dA}{dx} \right)^2 + \left( \frac{dA}{dy} \right)^2} \right\}, \quad (3)$$

where:  $M$  is the total magnetic field anomaly grid.

The outcome of SPI computations is presented in Figure 5.

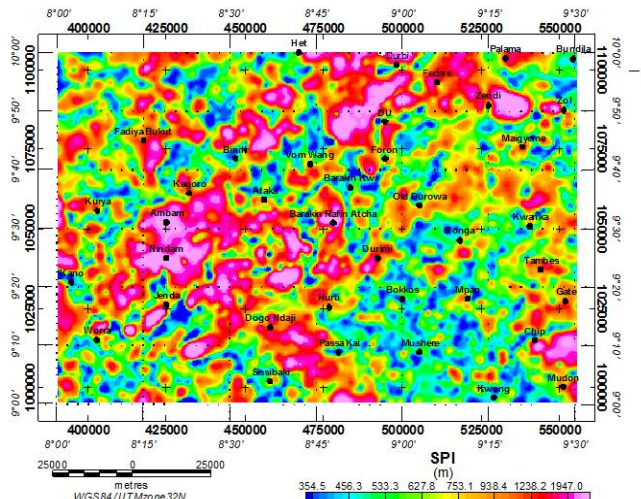


Figure 5. SPI results for the study region

## 2.2. Butterworth bandpass filter

The application of frequency-selective signal processing was achieved through a Butterworth bandpass filter, chosen for its maximally flat response in the bandpass region. This filtering approach effectively isolates specified frequency ranges while suppressing others, offering precise control over the filter's roll-off characteristics without altering the central wavenumber. The filter order can be adjusted to mitigate potential Gibbs phenomena, ensuring optimal signal preservation within the frequency band of interest. Unlike alternative filtering methods that may introduce bandpass ripples, the Butterworth filter's smooth response makes it particularly suitable for geophysical data processing where signal integrity is paramount. The Butterworth bandpass filter's transfer function,  $H(s)$ , is formulated based on its low-pass prototype and can be expressed as follows [2], [38], [39]:

$$H(s) = \frac{K}{\sqrt{1 + \left(\frac{S}{\omega_c}\right)^{2N}}}, \quad (4)$$

where:  $s = j\omega$  is the complex frequency variable;  $\omega_c$  is the cutoff frequency;  $N$  is the order of the filter;  $K$  is the gain at  $\omega = 0$ .

For a bandpass filter, the transfer function can be expressed as:

$$H(s) = \frac{Ks^{2N}}{\prod_{k=1}^N \left( s^2 + 2s \cos\left(\frac{(2k-1)\pi}{2N}\right) \omega_0 + \omega_0^2 \right)}. \quad (5)$$

The parameter  $\omega_0$  represents the central frequency of the bandpass filter. This filter was implemented using the Geosoft Oasis software, and the resulting output is shown in Figure 6. The filter order was carefully chosen to achieve an optimal trade-off between achieving sharp frequency cut-offs and minimizing ringing effects.

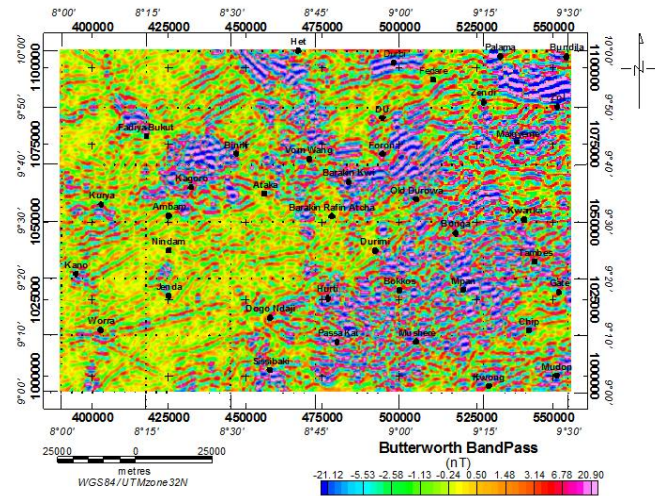


**Figure 6. Butterworth bandpass map for the study area**

Figure 6 was achieved by implementing a long wavelength cutoff of 4450 cyc/m and short wavelength cutoff of 1520 cyc/m. The map has successfully identified anomalous subsurface structures and emphasized their locations within the region.

### 2.3. Analytic signal (AS)

The analytic signal (AS) processing technique was employed as it combines both amplitude and phase information from magnetic anomalies, facilitating the identification of subtle magnetic signatures associated with lithological variations and geological boundaries [34], [40]. The AS technique has proven especially valuable in complex geological terrains where traditional magnetic interpretation methods may be limited by interference effects and varying magnetization directions [2], [33]. The interpretation of magnetic anomalies presents significant challenges due to the complex relationship between observed signals and their geological sources. Magnetic data interpretation is particularly complicated by horizontal displacements of anomalies relative to their sources (skewness), which occurs because geomagnetic field vectors and induced magnetization directions typically deviate from vertical orientations [33], [41].

The AS function, although not a directly measurable physical property, plays a crucial role in geophysical interpretation due to its independence from both the inducing field orientation and the magnetization direction. This unique characteristic ensures that bodies of similar geometry produce identical analytic signal responses. Additionally, the AS peaks are symmetric and are positioned directly above the edges of broader bodies or over the centres of narrower ones, providing valuable spatial information about subsurface structures [42]. AS is given by Equation (6):

$$A(x, y) = \sqrt{\left(\frac{\partial T}{\partial x}\right)^2 + \left(\frac{\partial T}{\partial y}\right)^2 + \left(\frac{\partial T}{\partial z}\right)^2}, \quad (6)$$

where:  $T$  is the observed field at  $x$  and  $y$ .

AS technique serves as a reliable tool for estimating the depth of magnetic sources, especially under the assumption of vertical contacts. Utilizing a straightforward amplitude half-width approach, this method achieves depth estimations with a typical accuracy of around 70%. A notable strength of the AS technique is its capacity to bypass the challenges often associated with conventional reduction-to-pole methods, which are hindered by uncertainties arising from the influence of natural remanent magnetization on the overall magnetization of the source. This capability makes the AS method a robust alternative for magnetic data interpretation, even in complex geological settings [2], [43]. Figure 7 illustrates the outcomes of the Analytic Signal (AS) computations, confirming its utility in scenarios where the magnetic properties of subsurface structures are either complex or insufficiently characterized.

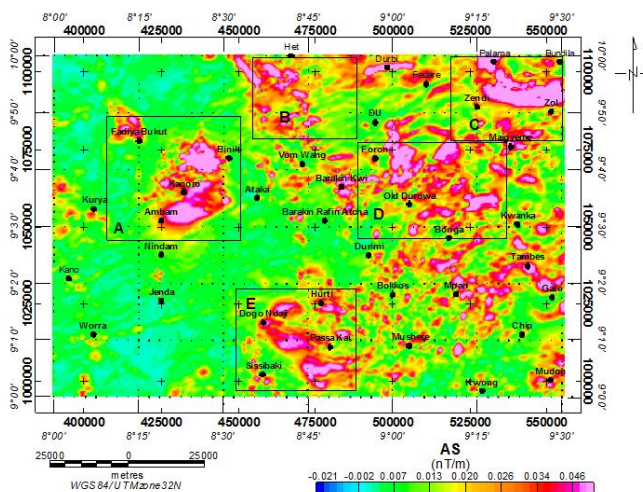


**Figure 7.** AS map of the study area, highlighting five strategic windows (A, B, C, D, E) selected at locations of suspected subsurface anomalies with potential mineralization

Rather than relying on absolute magnetic intensities, the AS technique emphasizes the anomaly's geometry, making it a robust and adaptable method for interpreting magnetic data. The ability of the AS method to effectively delineate potential mineralized subsurface geological structures, as further corroborated by Phase Symmetry (PS) analysis results, guided the selection of specific data windows (A, B, C, D, E) at key locations for additional processing. Subsequently, Euler Deconvolution (ED) and 3D magnetic data inversion were applied to these windows, enhancing the resolution and clarity of the final interpretations.

#### 2.4. Phase symmetry (PS) analysis

Phase symmetry is closely associated with the principle of phase congruency (PC), which quantifies the alignment of phase across multiple frequency components. Phase congruency occurs when various frequency components within a signal exhibit similar phase values, indicating a state of phase alignment. In regions of symmetry within an image or signal, the local phase remains consistent across different scales, resulting in elevated phase congruency levels.

The fundamental concept underlying phase symmetry analysis is mathematically defined by a series of key equations [44], starting with signal representation.

A signal  $I(x)$  can be broken down in terms of its local amplitude  $A(x)$  and local phase  $\phi(x)$  using the analytic signal:

$$I(x) = A(x) \cos(\phi(x)). \quad (7)$$

Phase congruency  $PC(x)$  at a point  $x$  can be calculated using:

$$PC(x) = \frac{\left( \sum_n W_n (\phi_n(x) - \phi_0(x)) \right) - \left| \sum_n W_n \sin(\phi_n(x) - \phi_0(x)) \right|}{\sum_n W_n} \quad (8)$$

where:  $\phi_n(x)$  is represents the phase at scale  $n$ ;  $W_n$  is a weighing function based on the amplitude;  $\phi_0(x)$  is the reference phase.

Phase symmetry  $PS(x)$  is calculated as a normalized measure of phase congruency, incorporating contributions from both positive and negative symmetries. It is defined as:

$$PS(x) = \frac{PC_+(x) + PC_-(x)}{2} \quad (9)$$

where:  $PC_+(x)$  and  $PC_-(x)$  correspond to the phase congruency values for positive and negative symmetries, respectively.

In summary, the phase congruency and phase symmetry measures describe how local phase information can be used to identify structural features within a signal. These parameters provide illumination- and contrast-invariant representations, making them highly effective for feature detection and image analysis.

The computed  $PS$  results are presented in Figure 8, while Figure 9 illustrates the outcomes for phase congruency.

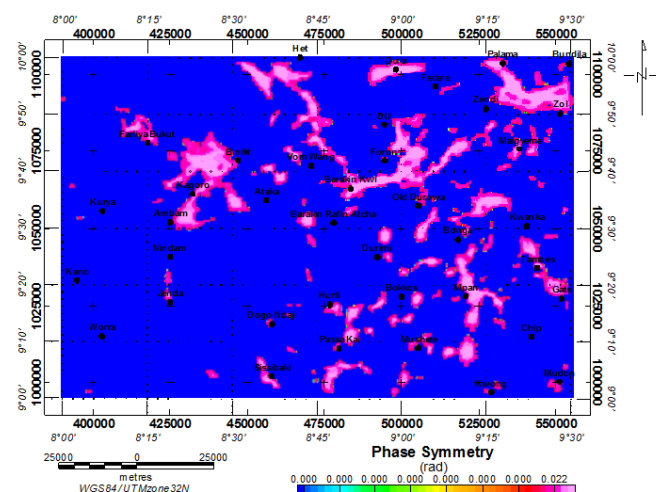


**Figure 8.** PS analysis of magnetic anomalies in the study area

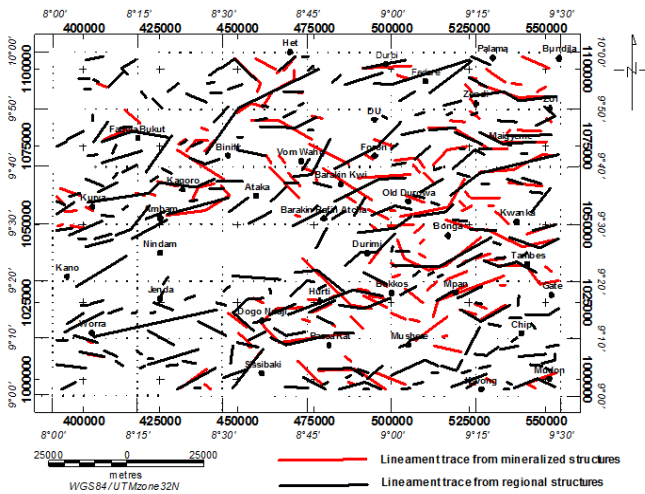


Figure 9. Lineament map from Phase Congruency showing the various subsurface trends within the region

## 2.5. Tilt derivative (TDR)

The TDR technique is instrumental in accentuating shallow features within geophysical datasets and mapping the boundaries of subsurface structures. This approach excels at identifying subtle anomalies and defining the edges of geological bodies. TDR is mathematically defined as the arctangent of the ratio of the vertical gradient to the horizontal gradient of a potential field. This dimensionless parameter reflects the angle formed between the total gradient vector and the horizontal plane, providing a robust tool for structural delineation [2], [45], [46]. TDR result is displayed in Figure 10.

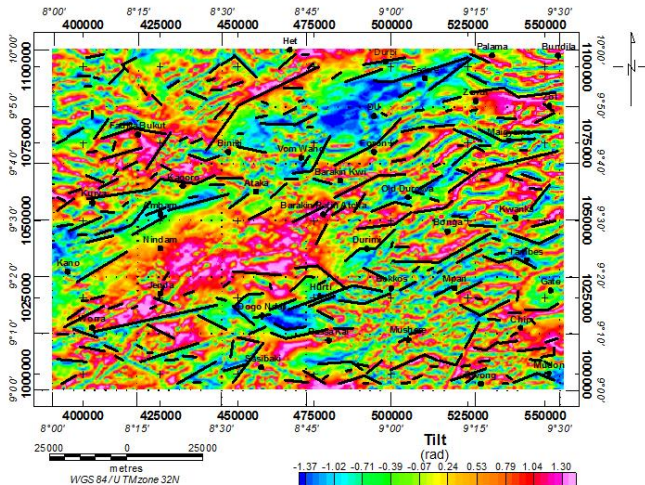


Figure 10. TDR map of the study area

## 2.6. Euler deconvolution (ED)

ED was utilized to analyze the residual magnetic data, providing insights into the depths and spatial positions of magnetic sources responsible for the observed anomalies. This approach, based on the second vertical derivative of the magnetic field, enabled the precise characterization and mapping of distinct magnetic sources such as faults, dykes, and mineralized zones.

The generalized 3D form of Euler's equation is expressed as Equation (10) [47], [48], [49]:

$$x \frac{\partial T}{\partial x} + y \frac{\partial T}{\partial y} + z \frac{\partial T}{\partial z} + \eta T = x_0 \frac{\partial T}{\partial x} + y_0 \frac{\partial T}{\partial y} + z_0 \frac{\partial T}{\partial z} + \eta b, \quad (10)$$

where:  $x, y, z$  are coordinates of a measuring point;  $x_0, y_0, z_0$  are coordinates of the source location whose total field is detected at  $x, y$ , and  $z$ ;  $b$  is a base level;  $\eta$  is a structural index (SI).

The SI represents an exponential factor that correlates with the rate of field decay over distance for a source with a specific geometry. The value of the SI is contingent upon the type of source body under investigation [48]. For instance,  $\eta = 0$  denotes a contact,  $\eta = 1$  signifies the top of a vertical dyke or the edge of a sill,  $\eta = 2$  corresponds to the center of a horizontal or vertical cylinder, and  $\eta = 3$  represents the center of a magnetic sphere or dipole [37], [47]. The implementation of Euler deconvolution is depicted in Figure 11 for a structural index of 1. Geosoft Oasis Montaj software [50] was used in the implementation of these concepts.

## 2.7. Euler deconvolution (ED)

The processed magnetic data were utilized to develop three-dimensional (3D) geological models, enabling the visualization and interpretation of subsurface structures associated with mineralization. Incorporating magnetic susceptibility contrasts facilitated the characterization of geological features and the delineation of potential mineralized zones, providing insights into the structural extent and spatial distribution of anomalies. The 3D modeling results are presented in Figure 12.

Pilkington [51] employed the Cauchy norm, as outlined by Sacchi and Ulrych [52], to tackle the 3D magnetic inversion problem. This method emphasizes the generation of sparse models by minimizing the number of non-zero parameters required to fit the observed data. Unlike constrained inversion techniques, which integrate explicit geological information such as drill hole data to guide the modeling process, Pilkington's approach is classified as geologically unconstrained [2]. This unconstrained method relies exclusively on magnetic data and mathematical algorithms, making it especially useful in scenarios where geological constraints are unavailable or when an unbiased interpretation of the magnetic anomalies is necessary. However, the lack of geological constraints may result in solutions that, while mathematically sound, might not fully align with known geological structures or properties in some cases.

## 3. Results and discussion

A direct correlation exists between geological complexities of a region and increased potential for mineral deposits within the region. The varied rock types, from magnetic-rich amphibolite and BIFs to relatively non-magnetic quartzite and schist, coupled with the structural complexity of the region, produced a diverse range of magnetic signatures that we utilized to delineate potential mineralization structures and zones in the study area. The structural geology of northern Nigeria's basement complex has been significantly shaped by extensive crustal deformation (Figure 2). This tectonic activity created numerous conduits and channels, facilitating the migration of mineralized solutions and magmatic intrusions throughout the rock formations.

As a consequence of these intricate geological events, the region has become a repository for diverse mineral deposits. The area boasts an impressive array of economically valuable resources, as illustrated in the mineral distribution map (Figure 3). These include metallic minerals (tin, iron ore, columbite, tantalite, wolframite, and beryl), industrial minerals

clay, kaolin/kaolinitic clay, mica, and talc), and gemstones (garnet and tourmaline). This remarkable mineral endowment has been well-documented in geological studies [53], [54] highlighting the region's significance as a mineral-rich terrain with substantial economic potential. Significant concentrations of columbite and tantalite minerals are noticed within the study area. At the northern locations of Rafin

Bawa, Fedare, Zendi and Wang, these minerals are traced to the younger granite complex of the region. Similar existence is noticed at the central (Dorowa Tsofo) and southern (Sissibaki) locations of the younger granite formation. The Precambrian basement with migmatite gneiss complex at the western regions of Kurya, Antan and Unguwar Kwasea locations, also hold significant record of these minerals.

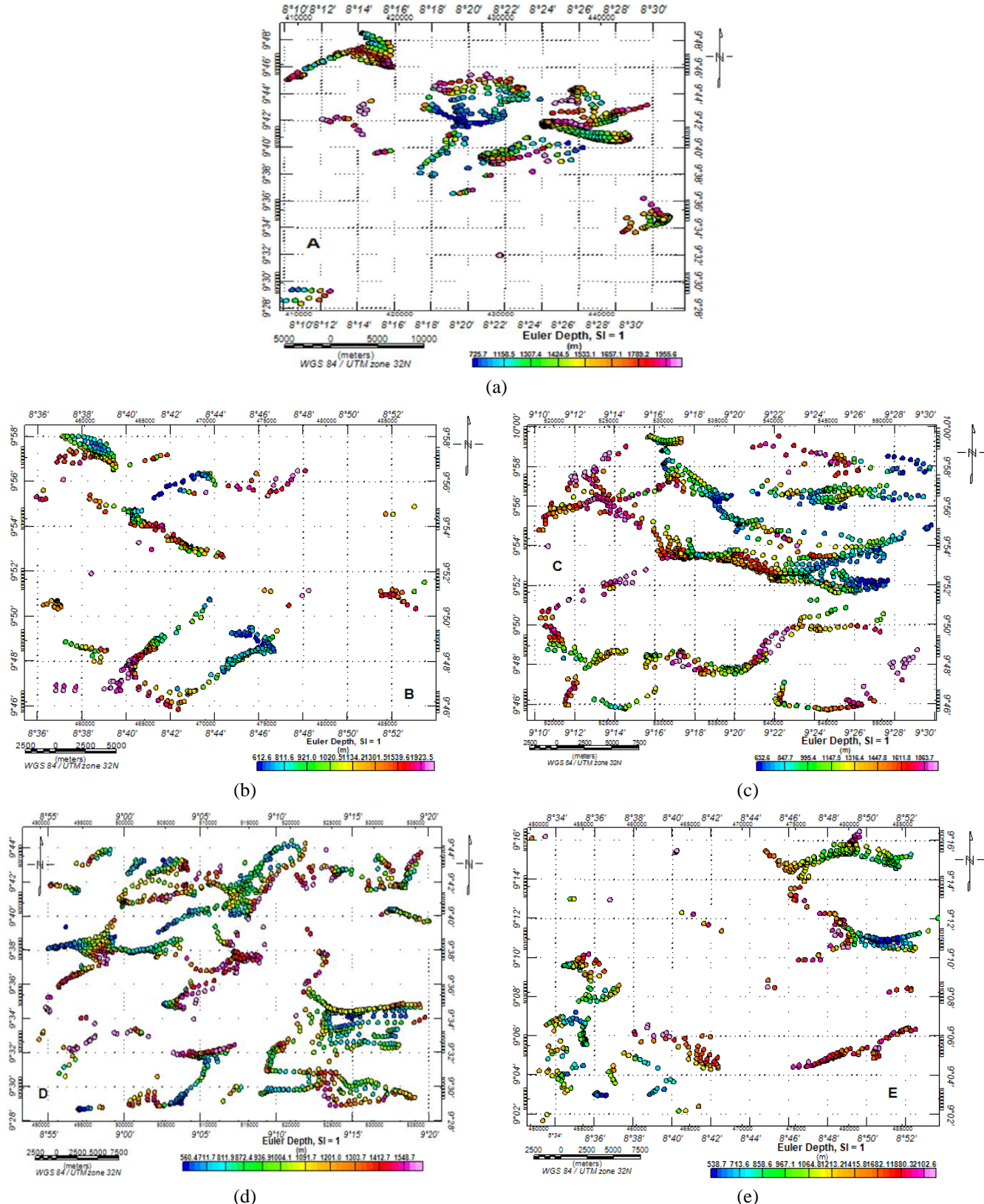


Figure 11. Euler depths solution for Windows A, B, C, D and E

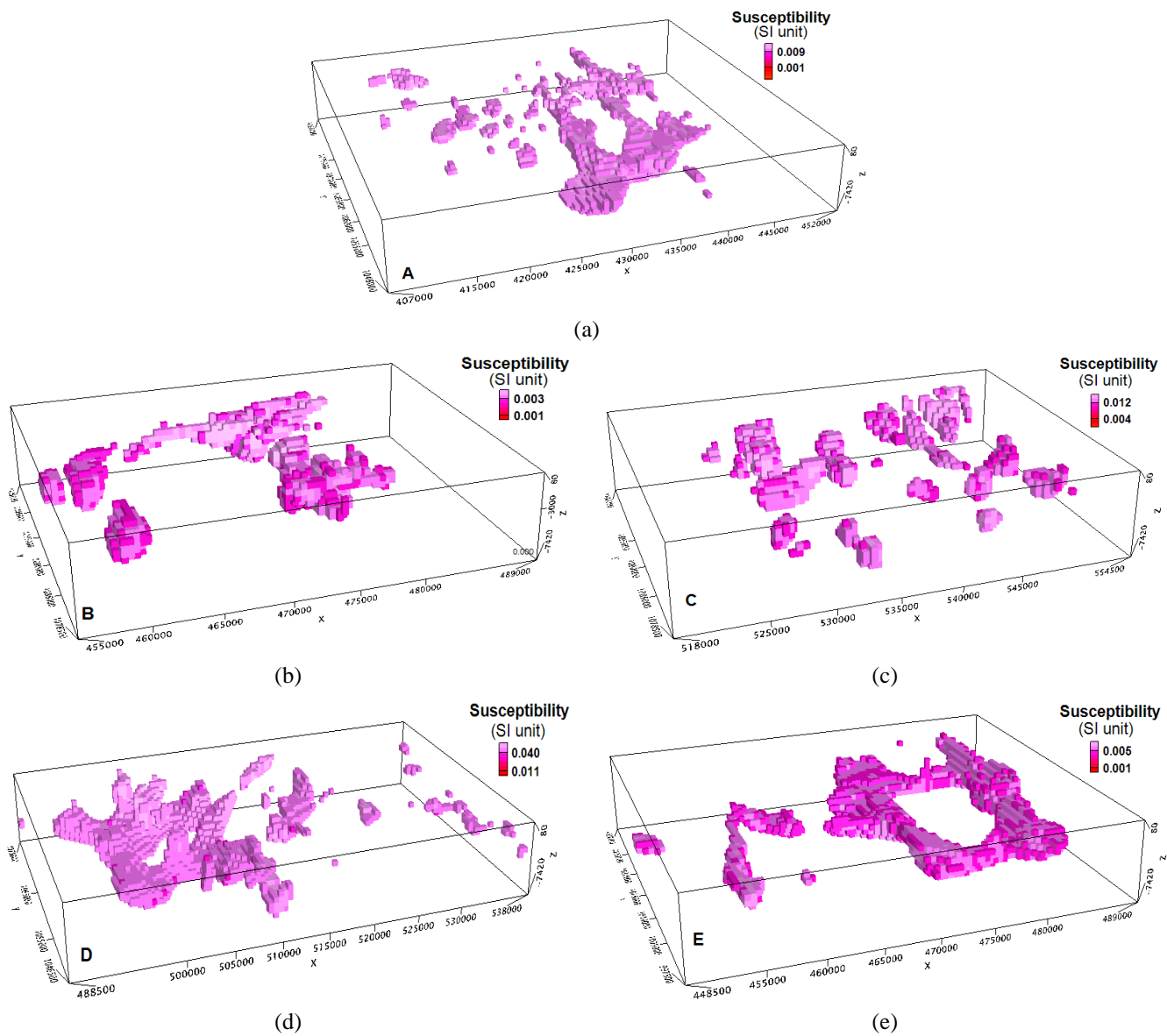


Figure 12. 3D magnetic inversion result for Windows A, B, C, D and E with r.m.s. error of 0.0001 nT

While tourmaline dominace is noted at the SW location of Ungwan Bahagn and Jenda towns, kaolin and kaolinitic clay dominates the northern and central towns of Foron, Ama, Barakin Rafin, and Fedare. These locations are on the granite and granite porphyry, and biotite granite of the Precambrian basement (Figure 2). Porphyritic granite complexes played vital roles in hosting the mineralized structures in the study area. Other minerals with significant presence (example, talc), are traced to the basalt's formation.

The residual magnetic anomaly map of the Kaduna-Nasarawa region (Figure 4) exhibits a significant range of magnetic intensities, varying from -115 to 91 nT. This broad range of values reflects the complex geology of the area and suggests the presence of diverse lithological units with varying magnetic susceptibilities. Observed magnetic contrasts are attributed to several geological factors that indicate potential zones of mineralization. The strongly positive magnetic anomalies (50-91 nT) correspond to the mafic rock body of basalt (Nindam location) and the felsic to intermediate Migmatite rocks of the Jenda, Chip, Zol and Kagoro locations. They potentially represent metamorphosed volcanic rocks or intrusive complexes with particular significance to

host the mineralization in the region. The elevated magnetic responses in these areas suggest the presence of deep-seated structures that may have facilitated mineral emplacement during the Pan-African orogeny.

Magnetite-rich banded iron formations (BIFs), which are common in the Precambrian terrain suggests potential for high-grade iron ore deposits in the study area. Moderate positive anomalies (0-50 nT) as seen at Ataka, Bokkos and Kano areas likely reflect amphibolite units within the migmatite-gneiss complex and also ferruginous quartzite, which may host stratabound iron deposits. Low-amplitude negative anomalies (-50 to 0 nT) may indicate granitic intrusions of the Older Granite suite, typically characterized by lower magnetic susceptibilities. Significant occurrences of ancient granite intrusions are observed within the crystalline basement complex of Nigeria, exhibiting diverse directional trends [3]. The Fedare, Du, Vom Wang, Ambam and Dogo Ndaji areas exhibits lower magnetic intensities (-110 to -10 nT), and locates mostly on the biotite granite. These zones are associated with the mica-rich biotite schists, kaolinitic clay deposits, and tourmaline-bearing pegmatites of the region. The moderate – lower magnetic signatures at these locations may indicate

zones of hydrothermal alterations, where primary magnetic minerals have been partially altered to less magnetic phases. These zones show correlation with kaolin deposits, talc occurrences (possibly indicating ultramafic protoliths), columbite and clay-rich weathering profiles.

The SPI result (Figure 5) further confirms the locations of identified subsurface sources and provides depth information to the sources. Our initial observation confirms the locations with suspected mineralized structures at the N, north-central, E and SE regions (Vom Wang, Barkin Rafin, Barakin Kwi, Mpan, Bokkos and Mushere locations) with shallow depths (350-470 m). Intermediate depths (500-720 m) are also confirmed for intermediate sources identified from the other techniques at Zendi, Zol, Du, Barakin Rafin Atcha, Durimi Passa Kai and Chip locations. These are regions with identified mineralized structures with hosting potentials for kaolin, clay, niobium, columbite, beryl, tantalite minerals and Tin ores. Near-surface metamorphic rocks often associates with clay and kaolin deposits and the shallow sources could represent weathered zones containing secondary mineralization. Shallow intrusive bodies, particularly pegmatite, could host rare-metal mineralization [18].

The application of the frequency domain filter that effectively isolates magnetic anomalies within specified wavelength ranges enabled the separation of geological features at varying depths and scale (Figure 6). Cut-off wavelengths were chosen based on the estimated depths of key geological features [58]. The high frequency components of the filtered data reveal near-surface geological features representing weathered zones potentially hosting kaolin in the central, western and southern regions (Ambam, Kagoro, Arna, Barakin Rafin, Foron and Fedare locations), and clay deposits at the Het, Mushere and Nasarawa locations. The near-surface geological features represent surficial expressions of mineralized structures [59]. Some linear features are also observed at the SW, W and NW regions. These are likely representative of shallow shear zones or weathered fault traces as earlier revealed by other techniques. They also show strong correlations with weathered zones which are typically enriched in secondary minerals. The deep sources (low-pass band) or low-frequency components hints on deep-seated intrusive bodies and large-scale features (basement configuration and deep magmatic centers). We recommend the regions where anomalies are mapped across multiple frequency bands as high priority targets for further mineral exploration. We also note that the coincidence of shallow and deep features may also indicate significant mineralization as observed in the SE and N regions.

The analytic signal results (Figure 7) also delineates the edges of magnetic sources, regardless of the ambient magnetic field direction and source magnetization [56]. Several distinctive features are observed in the AS map which points at possible mineralization structures in the KNPS. High amplitude anomalies ranging from 0.04 to 0.05 nT/m are noticeable mostly at the NE, NW, S, and SE regions. These anomalies are traced to the Basalt formation in the NE, Biotite granites in the N and NE, granite gneiss and migmatite formations in the S. They appear concentrated along geological contacts and structural boundaries as could be seen on the geologic and lineament maps, and could be associated with the mineralization in the region. The background values (generally below 0.13 nT/m) observed at the SW, parts of

NW and in-between the high amplitude anomalies in the eastern region represent areas of relatively homogeneous lithology which may mask deeper sources due to the AS sensitivity to shallow features. The high amplitude zones ( $>0.03$  nT/m) correlates strongly with magnetite-rich metamorphic rocks hosting garnet deposits (Mineral map – Kwi location). A strong correlation is also observed with the mafic intrusions at the NE and SW regions and they may be related to the columbite – tantalite mineralization at these locations. The moderate amplitude zones (0.015-0.03 nT/m) represents migmatitic gneiss with variable magnetic mineral content and are also of the metasedimentary units hosting mica and kaolin deposits. The low amplitude zones ( $<0.014$  nT/m) holds potential for rare-metal pegmatites and also indicates weathered zones favorable for clay mineral formation (observed at Het location in the north). Similar observations were documented by Omotunde et al. [57] at a location of similar geological setup. The columbite – tantalite deposits at the NE and SW regions are associated within the moderate AS amplitudes (0.014-0.03 nT/m) whereas the rare-metal pegmatites are characterized by low AS amplitudes ( $<0.01$  nT/m). The clay and kaolin deposits (central and southern regions) are found in weathered profiles over moderate amplitude sources and also associates with broad, low-amplitude AS zones in the NW and SE regions of the study area.

The pattern of anomalies observed in the phase symmetry (PS) results (Figure 8) suggest major subsurface intrusions. Strong continuous PS highs (northern region) represent major shear zones or faults as confirmed in the geologic map and earlier analysis. These features are significant as they often control the emplacement of rare-metal pegmatite containing columbite, tantalite and wolframite [60]. The complex, mottled textures of the PS output at the northern (Vom Wang, Foron, Fedare) and SE (Hurti, Bokkos, Bonca) indicate intense deformation or alteration in the region. These textural variations are crucial for identifying potential hosts for pegmatite mineralization [61]. Columbite, tantalite and wolframite occurrences at the S (Sissibaki) and NE (Fedare) regions show strong correlation with the edges of the rounded PS anomalies. Areas of low PS response at Kurya and Chip locations corresponds to the clay and kaolin deposits at the locations. These locations are traced to the migmatite formation. Low PS response at the SW region also corresponds to the tourmaline mineral presence at the location. These associations reflect the pegmatite and metamorphic origins of these minerals [18]. We suggest zones where the PS features are pronounced and with notable intersections, as priority targets, especially areas with complex PS textures.

Deeper depths (750-2000 m) have been obtained mostly at regions unsuspecting of mineralized subsurface intruded structures or suspected deep sources. This assertion is supported by results from the analytic signal, Butterworth band-pass and the PS evaluations. We believe these regions could host significant mineralize structures but at deeper depths, hence the weak anomaly signals from the near-surface evaluations. The deep sources are indications of basement structures, major shear zones and deep-seated granitic intrusions at the locations. The shallow depths (250-500 m) solutions show strong association with clay and kaolinic deposits in the SE and north-central regions. These industrial minerals are typically found in weathered zones of the basement complex.

There are also some correlation of the shallow depths (300-600 m) with surficial columbite – tantalite placer deposits at parts of the N, W, and S regions. In some instance, the deeper depth solutions (>1200 m) may indicate potential source regions for mineralizing fluids. We advise focus on areas with shallow SPI solutions for industrial minerals, weathered zones and above intermediate-depth magnetic sources for high-quality kaolin deposits [62], and areas where intermediate-depth solutions (700-1200 m) intersecting with known structural controls, for rare-metal mineralization.

There are also some secondary NW-SE trending structures (Fadiya Bukut, Hurti and Malgyme regions) and E-W trending discontinuities scattered all over the study area. The complex overlapping patterns in the features suggest multiple intrusive events and the sharp transition contact zones observed in the various amplitudes indicates lithological boundaries [45]. These trends have been corroborated by results from the phase congruency (PC) evaluations, superimposed on the tilt derivative map. Consequently, areas of high PC density at the NE, NW, SE, and southern regions of the study area indicates intense deformation. This is also evident in the geology map of the region. Zones of low PC density suggest more homogeneous lithology as observed at the SW region of the study area.

Integration of the tilt derivative with the PC analysis (Figure 9) show PC edges coinciding with the sharp tilt gradients (0.5-1.5 rad) evident at Kurya, Nindam, Passa Kai, Foron, Barakin Rafin and other locations. These interactions confirms some mapped structures on the geology map and also reveals subtle structures not apparent in the magnetic anomaly data. The high frequency, short-wavelength anomalies in the tilt derivative result (parts of NE, N, and SE regions) corresponds to near-surface metamorphic rocks in the KNPS and may indicate zones of hydrothermal alteration. These are potential areas for clay and kaolin deposits. This deduction is also observed on the mineral map of the area. The low frequency, long-wavelength features (parts of SW and NE regions) points to deeper and more extensive geological bodies (also observed on the geology map), and may represent basement structures or major intrusive complexes within the KNPS. Columbite – tantalite deposits are associated with sharp PC edges in the moderate magnetic anomaly zones, preferentially occurring along NE-SW trending PC features.

The intersections of the PC trends in Figure 9, indicates favorable structural settings for columbite-tantalite deposits. We interpret the broad, diffuse PC features at regions with concentrated PC and magnetic lows (S and NE regions) as been associated with the clay and kaolin deposits. Sharp tilt derivative gradients (southern Jenda, Mushere and Kwi) also indicates lithological contacts [55] and could be responsible for the mica mineralization along the pegmatite margins, clay deposits in the weathered contact zone as well as the garnet presence in the metamorphic aureoles.

We present results from the Tilt derivative (Figure 10) with superimposed trends from phase congruency (PC) computations. The superpositioning was performed for ease of direct comparisons. The patterns are consistently highlighted in both analyses, despite being derived through independent methods. Figure 10 presents the lineament map of the study area, exclusively illustrating the diverse subsurface trends across the region. Two unique trending were identified.

While the general trends were captured from the magnetic anomalies in the region, trending of the mineralized structures have also been captured with some interacting with the general trends of the study area. The tilt derivative map reveals several significant features in the study area. Primary NE-SW lineaments represent major shear zones related to the Pan-African orogeny and are associated with columbite-tantalite mineralization. Predominant linear features are observed at Jenda, Ambam, Dogo Ndaji – Hurti, and Foron regions.

Euler depth solutions from magnetic anomalies windows (A, B, C, D, and E) are shown in Figure 11. The Euler solutions reveal a multi-level distribution of magnetic sources. With our primary focus on delineating possible presence of dykes or sill structures ( $SI = 1$ ) in the study area, we interpret the clustering of solutions in the windows as indicative of dyke or sill structures or edges of these structures hosting minerals within the considered windows. The shallow sources (<500 m) corresponds to the weathered zones hosting clay, niobium, beryl, kaolin deposits (Windows B, C, D, and E) and shallow pegmatite bodies containing tourmaline and mica (Window C and E). These findings align with the work of Oruc and Salim [65], who noted similar depth distributions in the Precambrian terrains. We interpret the deeper sources (>500 m) as deep-seated intrusive bodies and possible ultramafic sources of mineralization (example, talc – NW region of Gidan Tagwai) and SE region (Mushere). Analysis of the spatial distribution of Euler solutions reveals several key patterns with linear clusters predominantly trending NE-SW (Windows A, B, D, and E). These are interpreted as dyke swarms or shear zones. The circular and rounded clusters characterized by concentric arrangements of solutions with elongations in the E-W, NE-SW trending (Windows A, C, D, and E) represents multiple structural indices and suggest complex geometry in the study area. This assertion is confirmed in the geology map and the 3D magnetic inversion results. These clusters may likely represent granitic intrusions hosting rare-metal pegmatite and metamorphic domes with potential for garnet and mica.

Insights into the structural framework has also been provided by the lineation of the Euler solutions. Linear alignments of solutions may represent fault systems and multiple depth ranges suggest deep rooted structures. These are key controls on mineralization particularly for the wolframite and tourmaline bearing pegmatite (Windows E and C), kaolin, and tin ore (Window B, D, and E). Similar structural controls were identified by Amigun et al. [66] and Abraham et al. [67]. Intrusive complexes characterized by clustered solutions with depths >600 m (Windows A, B, C, D, E), are also potential source regions for rare-metal pegmatite and hydrothermal mineralization. The Euler solutions realized have provided depth constraints to the magnetic lineaments identified in the tilt derivative map as some clusters of the solutions correlate with zones of high magnetic gradients and intersections of major structural features.

The 3D inversion results (Figure 12) reveal a complex distribution of magnetic susceptibility within the study area. The final representative structures realized in the 3D windows (Figure 12) were achieved by clipping susceptibilities of various units to leave-out the anomalous units. The models provide insights into the vertical distribution of potential mineralization. Suspected structures at Fadiya Bukut (Win-

dow A) at depths (350-1220 m) traces to possible subsurface structures hosting niobium, columbite, and tantalite minerals at the location. A major subsurface structure is mapped SE in Window A (eastern regions of Ambam – Anta – Ataka). This structure is significant in size and depths (1000-2500 m). This could represent deep-seated mineralized structure hosting the columbite, molybdenite and tin ores at the locations. Window B reveals intruded subsurface structures (200-1600 m) with possible mineralization of columbite, monazite, tantalite and clay. At the Palama – Zendi – Zol locations (Window C), significant intrusives have been noticed (170-200 m). These could represent possible kaolin/kaolinitic clay and tourmaline mineral hosts within the subsurface. Clay, kaolin and mica-rich pegmatites recorded at shallow mineralization in the windows are consistent with weathering – controlled deposits described by Salawu et al. [63].

A significant interconnected structure (400-3200 m) is captured in Window D and traces largely to the older basalts, porphyritic granite, biotite granite and the migmatite complexes. This is indicative of a significant subsurface mineralized structure at this location yet discovered, notwithstanding traces of tin ores noted at the Old Durowa location. Deep features (>1200 m) are characteristic of large, cohesive bodies of elevated susceptibility. With susceptibility values ranging from 0.02 to 0.08 SI, a greater percentage of these features are interpreted as major basement structures. Intermediate to deeper depth targets in Window E (150-3000 m) may be responsible for the columbite – tantalite, wolframite, garnet, feldspar, kaolin/kaolinitic clay, beryl, tin/nickel and clay minerals recorded at the location. These are analogous to deep mineral systems described by Denith et al. [64].

#### 4. Conclusions

The integrated analysis of high-resolution aeromagnetic data over the Kaduna-Nasarawa Precambrian Shield (KNPS) has provided significant insights into the region's mineral potential and structural framework. Through the application of multiple magnetic data enhancement techniques, our study has successfully delineated a complex network of mineralized structures at various depths, offering a comprehensive understanding of the region's mineral resources. The correlation between magnetic signatures and known mineral occurrences has validated our methodological approach while simultaneously revealing new prospective zones for exploration.

The residual magnetic anomaly patterns, ranging from -115 to 91 nT, reflect the diverse lithological units within the study area, with strongly positive anomalies corresponding to mafic rock bodies and intermediate values indicating potential rare-metal pegmatite. The integration of tilt derivatives with phase congruency analysis has proven particularly effective in identifying subtle structural features not apparent in the magnetic data, especially along the predominant NE-SW trending lineaments that control mineral emplacement in the region. These structural controls, further confirmed by analytic signal computations and 3D magnetic inversion modeling, demonstrate the critical relationship between tectonic activity and mineralization processes in the Nigerian Basement Complex.

Our depth analysis, combining source parameter imaging and Euler deconvolution, has established a clear vertical zonation of mineral deposits. Shallow sources (250-500 m) consistently correlate with industrial minerals, particularly

clay and kaolinitic deposits, while intermediate depths (500-720 m) host significant rare-metal pegmatite containing columbite, tantalite, and wolframite. The identification of deeper structures (>1200 m) suggests the presence of potential source regions for mineralizing fluids, offering new targets for deep exploration. The coincidence of anomalies across multiple frequency bands has highlighted priority exploration targets, particularly in areas where shallow and deep magnetic features intersect. The success of this integrated approach in mapping both known mineral occurrences and identifying new prospective zones demonstrates its efficacy for mineral exploration in complex Precambrian terrains. However, we recommend ground-truthing of the identified targets through detailed geological mapping and geochemical sampling to validate our interpretations.

Our study has contributed to the geological understanding of the Kaduna-Nasarawa Precambrian Shield and also provides a methodological framework for systematic mineral exploration in similar geological settings. The economic implications of our findings are significant, offering valuable guidance for targeted exploration efforts in the region. As Nigeria seeks to diversify its economy through the development of its solid mineral resources, the approach and results presented here represent a valuable contribution to achieving this national objective.

#### Author contributions

Conceptualization: EA, MA; Data curation: EA, ME; Formal analysis: AU, EA, II; Investigation: EA, AU; Methodology: EA, AU, MA, ME; Project administration: EA; Resources: EA, II, ME; Software: EA, II; Supervision: EA, ME; Validation: EA, AU; Visualization: EA; Writing – original draft: EA, MA, AU; Writing – review & editing: EA, ME, AU, II; All authors have read and agreed to the published version of the manuscript.

#### Funding

This research did not receive any specific grant from funding agencies in the public, commercial, or not-for-profit sectors.

#### Acknowledgements

To all the anonymous reviewers and the editor, we say thank you for your comments and contributions which improved the quality of our submission.

#### Conflicts of interests

The authors declare no conflict of interest.

#### Data availability statement

The original contributions presented in the study are included in the article, further inquiries can be directed to the corresponding author.

#### References

[1] Subari, Erlangga, B.D., Maryani, E., & Arifin, D.N. (2021). Potential utilization of quartz sand and kaolin from tin mine tailings for whiteware. *Mining of Mineral Deposits*, 15(3), 1-6. <https://doi.org/10.33271/mining15.03.001>

[2] Abraham, E.M., Uwaezuoke, A.E., & Usman, A.O. (2024). Geophysical investigation of subsurface mineral potentials in North-Central Nigeria: Implications for sustainable mining and development. *Geomechanics and Geophysics for Geo-Energy and Geo-Resources*, 10(1), 192. <https://doi.org/10.1007/s40948-024-00913-3>

[3] Abraham, E., Usman, A., Chima, K., Azuoko, G., & Ikeazota, I. (2024). Magnetic inversion modeling of subsurface geologic structures for mineral deposits mapping in southeastern Nigeria. *Bulletin of the Mineral Research and Exploration*, 173(173), 85-105 <https://doi.org/10.19111/bulletinofmre.1267876>

[4] Usman, A.O., Abraham, E.M., Ezeh, C.C., Azuoko, G., Augustine, I.C., Chima, J.C., & Obinna, C.A. (2024). Structural modeling of subsurface geologic structures in Anambra and adjoining Bida Basins using aeromagnetic data: Implications for mineral explorations. *Kuwait Journal of Science*, 52, 100307. <https://doi.org/10.1016/j.kjs.2024.100307>

[5] Abraham, E.M., Onwe, M.R., Usman, A.O., Gwazah, C.A., & Uchenna, M.E. (2022). Mapping of mineral deposits within granitic rocks by aeromagnetic data-a case study from Northern Nigeria. *Arabian Journal of Geosciences*, 15, 1656 <https://doi.org/10.1007/s12517-022-10947-0>

[6] Leão-Santos, M., Li, Y., & Moraes, R. (2015). Application of 3D-magnetic amplitude inversion, to iron oxidecopper-gold deposits, at low magnetic latitudes: A case-study from Carajás Mineral Province, Brazil. *Geophysics*, 80(2), B13-B22. <https://doi.org/10.1190/geo2014-0082.1>

[7] Obaje, N.G. (2009). The Benue Trough. *Geology and Mineral Resources of Nigeria*. Springer. 57. SBN 3-540-92684-4. <https://doi.org/10.1007/978-3-540-92685-6>

[8] NGSA (2022). Nigeria Geological Survey Agency - Geological Map of Nigeria.

[9] Ogezi, A.E. (1977). Geochemistry and Mineralization Potential of the Basement Complex Rocks of the Jos-Bukuru Complex, Nigeria. *Nigerian Mining Journal*, 4(2), 45-53.

[10] Rahaman, M.A. (1988). Recent advances in the study of the Basement Complex of Nigeria. *Precambrian Geology of Nigeria, Geological Survey of Nigeria*, 11-43.

[11] McCurry, P. (1976). The Geology of the Precambrian to Lower Paleozoic Rocks of Northern Nigeria: A Review. In C. A. Kogbe (Ed.), *Geology of Nigeria* (pp. 15-39). Elizabethan Publishing Company.

[12] Telford, W.M., Geldart, L.P., & Sheriff, R.E. (1990). *Applied Geophysics* (2nd ed.). Cambridge University Press. <https://doi.org/10.1017/CBO9781139167932>

[13] Woakes, M., Ajibade, A.C., & Rahaman, M.A. (1987). Some metallogenetic features of the Nigerian basement. *Journal of African Earth Sciences*, 6(5), 655-664. [https://doi.org/10.1016/0899-5362\(87\)90004-2](https://doi.org/10.1016/0899-5362(87)90004-2)

[14] Ugwu, S.A., Nwankwoala, H.O., & Agada, E.A. (2017). Structural Analysis and Aeromagnetic Interpretation of Spot Image for Mineral Potentials in the Jos-Plateau Area, North Central Nigeria. *African Journal of Basic & Applied Sciences*, 9(5), 303-310, <https://doi.org/10.5829/idosi.ajbas.2017.303.310>

[15] Ennih, N., & Liégeois, J. (2008). The boundaries of the West African craton, with special reference to the basement of the Moroccan metacratonic Anti-Atlas belt. *Geological Society, London, Special Publications*, 297, 1-17. <https://doi.org/10.1144/SP297.1>

[16] Caby, R. (2003). Terrane assembly and geodynamic evolution of central-western Hoggar: a synthesis. *Journal of African Earth Sciences*, 37(3-4), 133-159. <https://doi.org/10.1016/j.jafrearsci.2003.05.003>

[17] Dada, S.S. (2006). Proterozoic evolution of Nigeria. The Basement Complex of Nigeria and its mineral resources (A Tribute to Prof. M. A. O. Rahaman). Akin Jinad & Co. Ibadan, 29-44. <https://www.scirp.org/reference/referencespapers?referenceid=1425168>

[18] Garba, I. (2003). Geochemical discrimination of newly discovered rare-metal bearing and barren pegmatites in the Pan-African ( $600 \pm 150$  Ma) basement of northern Nigeria. *Applied Earth Science*, 112(3), 287-292. <https://doi.org/10.1179/037174503225011270>

[19] Adepoju, M. (2022). Structural control of ore mineralization in the southeastern margin of western Nigeria basement. *International Journal of Geosciences*, 13, 547-556. <https://doi.org/10.4236/ijg.2022.137029>

[20] Elueze, A.A. (1982). Geochemistry of the Ilesha granite-gneiss in the basement complex of southwestern Nigeria. *Precambrian Research*, 19(2), 167-177. [https://doi.org/10.1016/0301-9268\(82\)90057-2](https://doi.org/10.1016/0301-9268(82)90057-2)

[21] Ekwueme, B.N., & Kroner, A. (2006). Single zircon ages of migmatites in the Obudu Plateau, Cross River State, SE Nigeria. *Journal of African Earth Sciences*, 44(4-5), 403-407. <https://doi.org/10.1016/j.jafrearsci.2005.11.013>

[22] Adekoya, J.A. (1998). The geology and geochemistry of the Maru Banded Iron-Formation, northwestern Nigeria. *Journal of African Earth Sciences*, 27(2), 241-257. [https://doi.org/10.1016/S0899-5362\(98\)00059-1](https://doi.org/10.1016/S0899-5362(98)00059-1)

[23] Oyinloye, A.O. (2011). Geology and geotectonic setting of the basement complex rocks in south western Nigeria: Implications on provenance and evolution. *Earth and Environmental Sciences*, 98-117. <https://doi.org/10.5772/26990>

[24] Okonkwo, C.T., & Folorunso, I.O. (2013). Petrochemistry and geotectonic setting of granitic rocks in Aderan area, SW Nigeria. *Journal of Geography and Geology*, 5(1), 30. <https://doi.org/10.5539/jgg.v5n1p30>

[25] Ajibade, A.C., Woakes, M., & Rahaman, M.A. (1987). Proterozoic Crustal Development in the Pan-African Regime of Nigeria. In Kroner, A., (Ed.), *Proterozoic Lithospheric Evolution* (pp. 259-271). Washington DC, USA: American Geophysical Union.

[26] Odeyemi, I. (1993). A comparative study of remote sensing images of the structure of the Okemesi fold belt, Nigeria. *ITC Journal*, 1993(1), 77-81.

[27] Oluyide, P.O. (1988). Structural trends in the Nigerian basement complex. In: Oluyide, P.O., et al. (Eds.), *Precambrian Geology of Nigeria*. *Geological Survey of Nigeria*, 93-98.

[28] Anifowose, A.Y.B., & Borode, A.M. (2007). Photogeological study of the fold structure in Okemesi area, southwestern Nigeria. *Journal of Mining and Geology*, 43(2), 125-130. <https://doi.org/10.4314/jmg.v43i2.18872>

[29] Kinnaird, J.A. (1984). Contrasting styles of Sn-Nb-Ta-Zn mineralization in Nigeria. *Journal of African Earth Sciences*, 2(2), 81-90. [https://doi.org/10.1016/S0731-7247\(84\)80001-4](https://doi.org/10.1016/S0731-7247(84)80001-4)

[30] Okunlola, O.A., & Ocan, O.O. (2009). Rare Metal (Ta-Sn-Li-Be) Distribution in Precambrian Pegmatites of Keffi Area, Central Nigeria. *Nature and Science*, 7, 90-99.

[31] Ganguli, S.S., Pal, S.K., & Kumar, S.K.P. (2021). Insights into the crustal architecture from the analysis of gravity and magnetic data across Salem-Attur Shear Zone (SASZ), Southern Granulite Terrane (SGT), India: an evidence of accretional tectonics. *Episodes*, 44(4), 419 - 422. <https://doi.org/10.18814/epiugs/2020/020095>

[32] Abraham E., Itumoh O., Chukwu C., & Onwe R. (2018). Geothermal Energy Reconnaissance of Southeastern Nigeria from Analysis of Aeromagnetic and Gravity Data. *Pure and Applied Geophysics*, 176: 22-36. <https://doi.org/10.1007/s00024-018-2028-1>

[33] Nabighian, M.N., Grauch, V.J.S., Hansen, R.O., LaFehr, T.R., Li, Y., Peirce, J.W., & Ruder, M.E. (2005). The historical development of the magnetic method in exploration. *Geophysics*, 70(6), 33ND-61ND. <https://doi.org/10.1190/1.2133784>

[34] Rajagopalan, S. (2003). Analytic Signal vs. Reduction to Pole: solutions for low magnetic latitudes. *Exploration Geophysics*, 34(4), 257-262. <https://doi.org/10.1071/EG03257>

[35] Jain, S. (1988). Total magnetic field reduction-The pole or equator? a model study. *Canadian Journal of Exploration Geophysics*, 24(2), 185-192. Retrieved from [https://cseg.ca/wp-content/uploads/1988\\_12\\_Sudhir\\_J\\_magnetic\\_field\\_reduction.pdf](https://cseg.ca/wp-content/uploads/1988_12_Sudhir_J_magnetic_field_reduction.pdf)

[36] Leu, L.K. (1981). Use of reduction-to-the-equator process for magnetic data interpretation. *Geophysics*, 47, 445.

[37] Thurston, J.B., & Smith, R.S. (1997). Automatic conversion of magnetic data to depth, dip and susceptibility contrast using the SPITM method. *Geophysics*, 62, 807-813. <https://doi.org/10.1190/1.1444190>

[38] Proakis, J.G., & Manolakis, D.G. (2007). Digital Signal Processing: Principles, Algorithms, and Applications. Prentice Hall, Pearson.

[39] Oppenheim, A.V., & Schafer, R.W. (2009). Discrete-Time Signal Processing. Pearson Education.

[40] Usman, A.O., Nomeh, J.S., & Abraham, E.M. (2025). Subsurface structural mapping a tool in understanding the Geodynamics of Mineralization within the North?Central Precambrian Basement of Nigeria, using aeromagnetic dataset. *Earth Science Informatics*, 18, 169. <https://doi.org/10.1007/s12145-024-01492-3>

[41] Roest, W.R., Verhoef, J., & Pilkington, M. (1992). Magnetic interpretation using the 3D analytic signal. *Geophysics*, 57(1), 116-125. <https://doi.org/10.1190/1.1443174>

[42] Cooper, G. & Cowan, D. (2006). Enhancing potential field data using filters based on the local phase. *Computers and Geosciences*, 32(10), 1585-1591. <https://doi.org/10.1016/j.cageo.2006.02.016>

[43] Adebisi, W.A., Folorunso, I.O., Abubakar, H.O., Olatunji, S., & Olaojo, M.O. (2024). Delineating structural features related to hydrothermal alterations for possible mineralization in share area, Kwara State Nigeria using aeromagnetic data. *Indonesian Journal of Earth Sciences*, 4(2), A1265. <https://doi.org/10.52562/injoes.2024.1265>

[44] Kovesi, P. (1999). Image Features from Phase Congruency. *Videre: Journal of Computer Vision Research*, 1(3), 1-26. Retrieved from <https://www.cs.rochester.edu/u/brown/Videre/001/articles/v1n3001.pdf>

[45] Miller, H.G., & Singh, V. (1994). Potential field tilt-a new concept for location of potential field sources. *Journal of Applied Geophysics*, 32(2-3), 213-217. [https://doi.org/10.1016/0926-9851\(94\)90022-1](https://doi.org/10.1016/0926-9851(94)90022-1)

[46] Verduzco, B., Fairhead, J.D., Green, C.M., & Mackenzie, C. (2004). New insights into magnetic derivatives for structural mapping. *The Leading Edge*, 23(2), 116-119. <https://doi.org/10.1190/1.1651454>

[47] Reid, A.B., Allsop, J.M., Grauser, H., Millet, A.J., Somerton, I.N. (1990). Magnetic interpretation in 3D using Euler-Deconvolution. *Geophysics*, 55, 80-91. <https://doi.org/10.1190/1.1442774>

[48] Whitehead, N., & Musselman, C. (2005). Montaj Gravity/Magnetic interpretation: Processing, analysis, and visualization system, for 3-D inversion of potential field data, for Oasis montaj v6.1. Geosoft Inc. ON, Canada

[49] Thompson, D.T. (1982). Eulph: A new technique, for making computer-assisted, depth- estimates, from magnetic data, *Geophysics*, 47, pp. 31-37. <https://doi.org/10.1190/1.1441278>

[50] GEOSOFT (2007). Geosoft Oasis Montaj software. Version 8.3

[51] Pilkington, M. (2009). 3D magnetic data-space inversion with sparseness constraints. *Geophysics*, 74(1) P.L7-L15. <https://doi.org/10.1190/1.3026538>

[52] Sacchi, M.D., & Ulrych, T.J. (1995). High-resolution velocity gathers and offset space reconstruction: *Geophysics*, 60, 1169-1177. <https://doi.org/10.1190/1.1443845>

[53] Megwara, J.U., & Udensi, E.E. (2014). Structural analysis using aeromagnetic data: case study of parts of Southern Bida Basin, Nigeria and the surrounding basement rocks. *Earth science research*, 3(2), 27. <https://doi.org/10.5539/esp.v3n2p27>

[54] Dzukogi, A.N.A., & Bello, M.M. (2022). Aeromagnetic Data Analysis and Interpretations to Investigate Solid Mineral Potential in Part of Northwest Nigeria. *African Journal of Advances in Science and Technology Research*, 4(1), 125-138. Retrieved from <https://publications.afropolitanjournals.com/index.php/ajastr/article/view/171>

[55] Ajana, O., Udensi, E.E., Momoh, M., Rai, J.K., & Muhammad, S.B., (2014). Spectral Depths Estimate of Subsurface Structures in Parts of Borno Basin, Northeastern Nigeria, using Aeromagnetic Data. *IOSR Journal of Applied Geology and Geophysics*, 2, 55-60.

[56] Mekonnen, T.K. (2004). Interpretation and Geodatabase of Dykes Using Aeromagnetic Data of Zimbabwe and Mozambique. M.Sc. Thesis, ITC, Delft, 80 p.

[57] Salem, A., Ravat, D., Gamey, T.J., & Ushijima, K. (2002). Analytic signal approach and its applicability in environmental magnetic investigations. *Journal of Applied Geophysics*, 49(4), 231-244. [https://doi.org/10.1016/S0926-9851\(02\)00125-8](https://doi.org/10.1016/S0926-9851(02)00125-8)

[58] Omotunde, V.B., Olatunji, A.S., & Abdus-Salam, M.O. (2020). Rare Earth Elements Assessment in the Granitoids of Part of Southwestern Nigeria. *European Journal of Environment and Earth Sciences*, 1(5). <http://doi.org/10.24018/ejgeo.2020.1.5.79>

[59] Goodenough, K.M., Schilling, J., Jonsson, E., Kalvig, P., Charles, N., Tuduri, J., Deady, E.A., Sadeghi, M., Schiellerup, H., Müller, A., Bertrand, G., Arvanitidis, N., Eliopoulos, D.G., Shaw, R.A., & Thrane, K., Keulen, N. (2016). Europe's Rare Earth Element Resource Potential: An Overview of REE Metallogenic Provinces and Their Geodynamic Setting. *Ore Geology Reviews*, 72, 838-856. <https://doi.org/10.1016/j.oregeorev.2015.09.019>

[60] Aliyu, A., Lawal, K.M., Abubakar, L.Y., Dada, I., & Olayinka, A. (2020). Geomagnetic Studies of Pegmatite Mineralization at Lema and Ndeji North-Central, Nigeria. *Journal of Mining and Geology*, 56(1), 81-89.

[61] Yunusa, A., Hong, H., Salim, A., Amam, T., Liu, C., Xu, Y., Zuo, X., & Li, Z. (2024). Mineralogical Characterization and Geochemical Signatures of Supergene Kaolinitic Clay Deposits: Insight of Ropp Complex Kaolins, Northcentral Nigeria. *Minerals*, 14(9), 869. <https://doi.org/10.3390/min14090869>

[62] Nasuti, Y., & Nasuti, A. (2018). NTilt as an improved enhanced tilt derivative filter for edge detection of potential field anomalies. *Geophysical J. International*, 214(1), 36-45, <https://doi.org/10.1093/gji/ggy117>

[63] Oruc, B., & Selim, H.H. (2011). Interpretation of Magnetic Data in the Sinop Area of Mid Black Sea, Turkey, Using Tilt Derivative, Euler Deconvolution and Discrete Wavelet Transform. *Journal of Applied Geophysics*, 74, 194-204. <https://doi.org/10.1016/j.jappgeo.2011.05.007>

[64] Amigun, J.O., Sanusi, S.O., & Audu, L. (2022). Geophysical characterisation of rare earth element and gemstone mineralisation in the Ijero-Aramoko pegmatite field, southwestern Nigeria. *Journal of African Earth Sciences*, 104494. <https://doi.org/10.1016/j.jafrearsci.2022.104494>

[65] Abraham, E.M., Nkitnam, E.E., & Itumoh, O.E. (2020). Integrated geophysical investigation of recent earth tremors in Nigeria using aeromagnetic and gravity data. *Environ Monit Assess*, 192:352 <https://doi.org/10.1007/s10661-020-08339-6>

[66] Salawu, N.B., Omosanya, K.O.L., Eluwole, A.B., Saleh, A., & Adebiyi, L.S. (2023). Structurally-controlled Gold Mineralization in the Southern Zuru Schist Belt NW Nigeria: Application of Remote Sensing and Geophysical Methods. *Journal of Applied Geophysics*, 211, 104969. <https://doi.org/10.1016/j.jappgeo.2023.104969>

[67] Dentith, M., Yuan, H., Johnson, S., Murdie, R., & Piña-Varas, P. (2018). Application of deep-penetrating geophysical methods to mineral exploration: Examples from Western Australia. *Geophysics*, 83(3), <https://doi.org/10.1190/geo2017-0482.1>

## Сирек металды минералданудың құрылымдық бақылауы: Нигерияның кристалды іргетасындағы экономикалық кен орындарының терең картасын жасау

Э. Абрахам<sup>1\*</sup>, М. Абдульфарадж<sup>2</sup>, М. Эметере<sup>1</sup>, А. Усман<sup>1</sup>, И. Икеазота<sup>1</sup>

<sup>1</sup>Алекс Эквуземе федералды университеті, Икво, Нигерия

<sup>2</sup>Абдулазиз университеті, Джидда, Сауд Арабиясы

<sup>2</sup>Боуэн университеті, Иво, Нигерия

\*Корреспонденция үшін автор: [ema.abraham@funai.edu.ng](mailto:ema.abraham@funai.edu.ng)

**Аннотация.** Бұл зерттеудің мақсаты минералдық-барлау жұмыстары үшін перспективалы аймақтарды анықтау және Кембрій алдындағы террандар шегінде минералдану процестерін түсінуді терендіту болып табылады. Жоғары дәлдіктерін аэромагниттік деректер аналитикалық сигналды, көлбекеу туынды өрісті, фазалық симметрияны, көз параметрлерін бейнелеуді, Баттеруорттың жолақтың сүзуін, магниттік ауытқулардың үш өлшемді инверсиясын және Эйлердің деконволюциясын коса алғанда, біріктірілген геофизикалық әдістер кешенін қолдану арқылы талданды. Бұл әдістер жер асты құрылымдарын боліп көрсетуге, олардың кеңістіктік таралуын, пайда болу терендігін және пайдалы қазбалардың көріністерімен байланысын анықтауга мүмкіндік берді. Нәтижелер минералды заттардың енгізілуін бақылайтын негізгі сыйысу аймақтары мен ақаулы жүйелерге сәйкес келетін солтүстік-шығыс және солтүстік-батыс кеңеюінің сыйықтық аймақтарының болуын көрсетті. Таяз бұлактар (250-500 м) саз сияқты өнеркәсіптік минералдармен байланысты; құрамында сирек кездесетін металл пегматиттері бар аралық тереңдіктер (500-720 м) колумбит-танталит және вольфрамит; ал терең құрылымдар (>1200 м) минералданатын сұйықтықтардың пайда болуының ықтимал аймақтарын көрсетеді. Аналитикалық сигналдың жоғары амплитудалық ауытқулары (0.04-0.05 нТ/м) геологиялық контактілермен және құрылымдық шекаралармен сәйкес келеді, мүмкін минералдану аймақтарын белгілейді. Бұл зерттеу аймақтың жер асты минералданған құрылымдарын зерттеуге бағытталған алғашқы кешенде жұмыс болып табылады. Геофизикалық әдістер кешенін қолдану бүрүн көрсетілмеген құрылымдық ерекшеліктерді анықтауга және минералданған аймақтардың тік үздіксіздігін растауга мүмкіндік берді. Жартылай алынған нәтижелер мақсатты геологиялық барлау жұмыстары үшін құнды түсініктер бере отырып және кристалдық іргетас шегінде колумбит-танталит, вольфрамит, каолин және басқа да ойластырылған минералдарды іздеудің дәлірек және үнемді стратегияларын әзірлеуге ықпал ететін, экономикалық маңызы бар кен орындарын терең бағдарланған картага түсіруді камтамасыз етеді.

**Негізгі сөздер:** магниттік деректер, пайдалы қазбаларды барлау, тереңдік, құрылымдық бақылау, тау-кен, кристалдық іргетас.

## Структурный контроль редкометалльной минерализации: глубинное картирование экономических месторождений в кристаллическом фундаменте Нигерии

Э. Абрахам<sup>1\*</sup>, М. Абдульфарадж<sup>2</sup>, М. Эметере<sup>1</sup>, А. Усман<sup>1</sup>, И. Икеазота<sup>1</sup>

<sup>1</sup>Федеральный университет Алекса Эквуземе, Икво, Нигерия

<sup>2</sup>Университет Абдулазиза, Джидда, Саудовская Аравия

<sup>2</sup>Университет Боуэн, Иво, Нигерия

\*Автор для корреспонденции: [ema.abraham@funai.edu.ng](mailto:ema.abraham@funai.edu.ng)

**Аннотация.** Цель данного исследования заключается в выявлении перспективных зон для минералого-разведочных работ и углублении понимания процессов минерализации в пределах докембрийских террейнов. Высокоточные аэромагнитные данные были проанализированы с использованием комплекса интегрированных геофизических методов, включая аналитический сигнал, наклонное производное поле, фазовую симметрию, изображение параметров источников, полосовую фильтрацию Баттервортса, трёхмерную инверсию магнитных аномалий и деконволюцию Эйлера. Эти методы позволили выделить подповерхностные структуры, определить их пространственное распределение, глубины залегания и взаимосвязь с проявлениями полезных ископаемых. Результаты показали наличие линейных зон северо-восточного и северо-западного простиляний, соответствующих главным зонам сдвига и разломным системам, контролирующими внедрение минерального вещества. Неглубокие источники (250-500 м) связаны с промышленными минералами, такими как глина; промежуточные глубины (500-720 м) с редкометалльными пегматитами, содержащими колумбит-танталит и вольфрамит; тогда как глубинные структуры (>1200 м) указывают на потенциальные области зарождения

минерализующих флюидов. Высокоамплитудные аномалии аналитического сигнала (0.04-0.05 нТ/м) совпадают с геологическими контактами и структурными границами, обозначая зоны возможной минерализации. Данное исследование представляет собой первую комплексную работу, направленную на изучение подповерхностных минерализованных структур региона. Применение комплекса геофизических методов позволило выявить ранее неотражённые структурные особенности и подтвердить вертикальную непрерывность минерализованных зон. Полученные результаты обеспечивают глубинно-ориентированное картирование экономически значимых месторождений, предоставляя ценные сведения для целенаправленных геологоразведочных работ и способствуя разработке более точных и экономически эффективных стратегий поисков колумбит-танталита, вольфрамита, каолина и других промышленных минералов в пределах кристаллического фундамента.

**Ключевые слова:** магнитные данные, разведка полезных ископаемых, глубины, структурный контроль, горное дело, кристаллический фундамент.

#### Publisher's note

All claims expressed in this manuscript are solely those of the authors and do not necessarily represent those of their affiliated organizations, or those of the publisher, the editors and the reviewers.